Earth and Planetary Science Letters 458 (2017) 263–272

Contents lists available at ScienceDirect

Earth and Planetary Science Letters

www.elsevier.com/locate/epsl

Thermal evolution of Earth with magnesium precipitation in the core

Joseph G. O'Rourke [a,*], Jun Korenaga [b], David J. Stevenson [a]

[a] Division of Geological and Planetary Sciences, California Institute of Technology, Pasadena, CA 91125, USA
[b] Department of Geology and Geophysics, Yale University, New Haven, CT 06520, USA

A R T I C L E I N F O

Article history:
Received 7 June 2016
Received in revised form 14 September 2016
Accepted 27 October 2016
Available online 14 November 2016
Editor: C. Sotin

Keywords:
Earth, interior
magnetic field
mantle convection
heat-flow scaling
thermal budget

A B S T R A C T

Vigorous convection in Earth's core powers our global magnetic field, which has survived for over three billion years. In this study, we calculate the rate of entropy production available to drive the dynamo throughout geologic time using one-dimensional parameterizations of the evolution of Earth's core and mantle. To prevent a thermal catastrophe in models with realistic Urey ratios, we avoid the conventional scaling for plate tectonics in favor of one featuring reduced convective vigor for hotter mantle. We present multiple simulations that capture the effects of uncertainties in key parameters like the rheology of the lower mantle and the overall thermal budget. Simple scaling laws imply that the heat flow across the core/mantle boundary was elevated by less than a factor of two in the past relative to the present. Another process like the precipitation of magnesium-bearing minerals is therefore required to sustain convection prior to the nucleation of the inner core roughly one billion years ago, especially given the recent, upward revision to the thermal conductivity of the core. Simulations that include precipitation lack a dramatic increase in entropy production associated with the formation of the inner core, complicating attempts to determine its age using paleomagnetic measurements of field intensity. Because mantle dynamics impose strict limits on the amount of heat extracted from the core, we find that the addition of radioactive isotopes like potassium-40 implies less entropy production today and in the past. On terrestrial planets like Venus with more sluggish mantle convection, even precipitation of elements like magnesium may not sustain a dynamo if cooling rates are too slow.

1. Introduction

The dynamo created in Earth's liquid outer core has survived for billions of years. Paleomagnetic studies of unmetamorphosed rocks with ages near 3.45 Gyr unambiguously show that the strength of Earth's global magnetic field at that time was at least half its present-day value (e.g., Tarduno et al., 2010; Biggin et al., 2011). No rocks of sufficiently low metamorphic grade have been found from earlier epochs, so the question of whether our magnetic field is even older remains unanswered. Recently, detrital zircon crystals found in the Jack Hills of Western Australia were proposed to record field intensities of modern magnitudes (Tarduno et al., 2015). These data are controversial, however, because zircon-bearing rocks in the Jack Hills may have suffered pervasive remagnetization related to the emplacement of a nearby igneous province (e.g., Weiss et al., 2015). In any case, how to power convection in the core and thus a dynamo for the vast majority of Earth's history remains one of the most pressing puzzles in geophysics.

Thermal convection in the core is possible if the heat flow across the core/mantle boundary (CMB) exceeds the rate at which heat is conducted along an adiabatic temperature gradient (e.g., Stevenson, 2003). Over the past few years, some theoretical calculations (e.g., de Koker et al., 2012; Pozzo et al., 2012) and diamond-anvil cell experiments (e.g., Gomi et al., 2013; Seagle et al., 2013; Ohta et al., 2016) have indicated that the thermal conductivity of the core's iron-rich alloy is a factor of two to three larger than prior estimates. The conductive heat flux is ∼10–15 TW at present according to these new values. However, countervailing evidence from high-pressure experiments that the previous, low values are actually correct has also been presented recently, so debate over this issue will likely continue (Konôpková et al., 2016).

Cooling rates approaching twice the conductive heat flux have been suggested as the minimum required to compensate for Ohmic dissipation (e.g., Stelzer and Jackson, 2013). But this dissipation mainly occurs at high harmonic degree and its scaling with dipole field strength is uncertain. Since the dissipation due to the low harmonics alone is far less than the actual heat flow, maintaining the observed field with a heat flow only mildly in excess of conduction along the adiabat is possible in principle. In any case, the actual CMB heat flow of ∼5–15 TW estimated from seis-

* Corresponding author.
E-mail address: jorourke@caltech.edu (J.G. O'Rourke).

http://dx.doi.org/10.1016/j.epsl.2016.10.057
0012-821X/

mology and mineral physics (e.g., Lay et al., 2008) may be only marginally sufficient to sustain the dynamo by thermal convection alone. Fortunately, the dynamic chemistry of the core yields additional sources of energy.

The exclusion of light elements from the solidifying inner core provides enough compositional buoyancy to drive convection today. Once compositional buoyancy is present, the heat flow out of the core need not exceed conduction along the adiabat (i.e., convection can even carry heat downwards). In practice, models with a growing inner core also benefit from the significant release of latent heat and accordingly require less rapid cooling. Conventional calculations have indicated that the inner core nucleated roughly one billion years ago (e.g., Labrosse et al., 2001). The age of the inner core is several hundred million years less in models with increased CMB heat flow and thus faster cooling/freezing to accommodate the revised values for thermal conductivity (e.g., Nimmo, 2015; Labrosse, 2015).

The energy available for dissipation in dynamo generation dramatically increases once the inner core forms, which might imply a larger magnetic field according to scaling laws where the buoyancy flux determines the global field strength (e.g., Christensen, 2010). In some canonical models, the inner core thus prevents the dynamo from turning off (e.g., Stevenson et al., 1983), but these models do not explain the current total heat flow of Earth. Biggin et al. (2015) claimed to observe an increase in Earth's dipole moment associated with the formation of the inner core in the Mesoproterozic. Given the relevant experimental and statistical uncertainties, however, the available data are arguably consistent with roughly constant field intensities throughout the Precambrian (e.g., Smirnov et al., 2016).

O'Rourke and Stevenson (2016) proposed the precipitation of magnesium-bearing minerals as an alternative power source. One or two weight percent of magnesium can partition into the core in the high-temperature aftermath of giant impacts during Earth's accretion according to earlier calculations (Wahl and Militzer, 2015) and subsequent diamond-anvil cell experiments (Badro et al., 2016). Because its solubility in iron alloy is strongly-temperature dependent, subsequent cooling quickly saturates the core in magnesium. Elements like aluminum and calcium may have similar thermodynamic properties (Badro et al., 2016), but their abundances are relatively small. Transporting magnesium-rich oxide or silicate across the CMB provides an order-of-magnitude more gravitational energy than freezing an equivalent mass of the inner core. Precipitation drives vigorous, compositional convection before the nucleation of the inner core, even without vastly higher CMB heat flow than today. O'Rourke and Stevenson (2016), however, only calculated the CMB heat flow implied by a constant rate of entropy production for the dynamo. In reality, mantle dynamics control CMB heat flow, so entropy production should vary over time.

The purpose of this paper is to describe simple models of Earth's thermal evolution that are consistent with the observed longevity of the dynamo. First, we describe how we couple a one-dimensional model of the core to simple scaling laws for mantle dynamics. We next identify which parameters control the amount of power available for the dynamo throughout geologic time. Specifically, we focus on the rheology of the boundary layer at the base of the mantle and the abundance of radioactive isotopes like potassium-40 in the core. After presenting representative simulations, we discuss the limitations of our model for early Earth history and the implications for other planets.

2. Theoretical formulation

In this section, we present a parametrized model for the coupled evolution of Earth's core and mantle. Fig. 1 shows the simplified structure with which we calculate thermal histories. Key

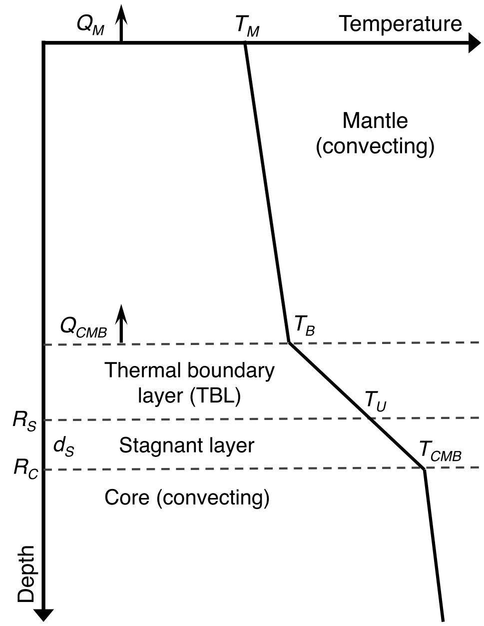

Fig. 1. Cartoon showing the assumed thermal structure of Earth and the key parameters tracked during simulations of Earth's evolution. The temperature gradients and vertical dimensions of each layer are not to scale.

Table 1
List of key parameters tracked during simulations of Earth's thermal evolution and their definitions.

Term	Definition
Q_M	Heat flow from the mantle
Q_{CMB}	Heat flow from the core
Q_R	Radiogenic heating in the core
Q_S	Secular cooling of the core
Q_P	Gravitational energy release from precipitation
Q_G	Gravitational energy release from the inner core
Q_L	Latent heat associated with the inner core
H_M	Radiogenic heating in the convecting mantle
T_M	Potential temperature of the mantle
T_B	Basal temperature of the convecting mantle
T_U	Temperature at the top of the stagnant layer
T_{CMB}	Temperature of the uppermost core
T_I	Temperature at the inner core boundary
R_I	Radius of the inner core
E_K	Entropy production associated with conduction
E_ϕ	Entropy production available for the dynamo

model parameters are listed in Table 1. As in nearly all models of core history for the past fifty years, we assume that the core is sufficiently low viscosity that the convective state is extremely close to an isentropic and homogeneous state, except in thin boundary layers (e.g., Stevenson, 1987). Although most previous studies (e.g., Stevenson et al., 1983; Buffett, 2002) only consider a thermal boundary layer at the base of the mantle, we allow for the existence of a stagnant layer that may not participate in convection because it is compositionally dense (Hernlund and McNamara, 2015), possibly the solidified remnant of a basal magma ocean (e.g., Labrosse et al., 2007). The existence of this distinct chemical layer could explain why the thermal excess associated with mantle plumes may be less than half the total temperature contrast across the CMB (e.g., Farnetani, 1997). Because our primary focus is how mantle dynamics affect the evolution of the core, we do not model the dynamics of the crust and lithosphere in detail. Finally, we present simulations that demonstrate the effects of varying key parameters.

Table 2
Values of parameters held fixed in our simulations. Other constants used to simulate the evolution of the mantle and to calculate the terms in the energy and entropy balances of the core were taken without modification from Korenaga (2006) and Labrosse (2015) unless otherwise indicated. References: [1] Christensen (1985), [2] Tang et al. (2014), [3] Korenaga (2005), and [4] Labrosse (2015).

Term	Definition	Value	Units	Ref.
C_M	Specific heat capacity of the mantle	4.5×10^{27}	J	[1]
k_M	Thermal conductivity in the stagnant layer	5	$\mathrm{W\,m^{-1}\,K^{-1}}$	[2]
$\eta_B(T_{ref})$	Mantle viscosity at reference temperature	2×10^{21}	Pa s	[3]
T_{ref}	Reference temperature for mantle viscosity	2500	K	[3]
$k_C(0)$	Thermal conductivity at the core's center	163	$\mathrm{W\,m^{-1}\,K^{-1}}$	[4]
L_p	Length scale for density profile in the core	8049	km	[4]
A_p	Constant for density profile in the core	0.4835		[4]
A_k	Constant for conductivity profile in the core	2.39		[4]
dT_m/dP	Liquidus slope at the inner core boundary	9	$\mathrm{K\,GPa^{-1}}$	[4]

2.1. Evolution of the mantle

The governing equation here is the global energy balance for the mantle (e.g., Christensen, 1985):

$$C_M \frac{dT_M(t)}{dt} = H_M(t) - Q_M(t) + Q_{CMB}(t), \tag{1}$$

where C_M is the heat capacity of the entire mantle, T_M is the potential temperature of the mantle, H_M is the radiogenic heating in the convecting mantle, Q_M is the heat flow out of the surface from mantle convection, and Q_{CMB} is heat flow across the core/mantle boundary. Heat-producing elements are partially sequestered in the continental crust, so H_M is less than the present-day heat production of the bulk silicate Earth. Table 2 lists the values we adopt for parameters like C_M that are generally fixed in our simulations.

At present, how to calculate Q_M remains quite controversial. Conventional scalings for Q_M assume that the mantle behaves like a simple convecting system in which hotter temperature yields an increased vigor of convection and thus heat flow. But there is a well-known problem with these scalings that arises when the convective Urey ratio, $Ur(t) = H_M(t)/Q_M(t)$, is considered (Christensen, 1985). Integrating Eq. (1) backwards in time yields unrealistically high values of T_M unless the present-day $Ur(t_0) \sim 0.75$. Robust geochemical constraints, however, imply that $Ur(t_0) \sim 0.2$ to 0.4 in reality (e.g., Korenaga, 2008; Lay et al., 2008).

Using the realistic Urey ratio in simulations of Earth's evolution produces a "thermal catastrophe" in which calculated mantle temperatures before ~2–3 Ga rapidly exceed petrological constraints (e.g., Herzberg et al., 2010). To avoid this problem, we calculate Q_M as a function of T_M following Korenaga (2006). This simple formulation is sufficient for the purposes of this study and is consistent with fully dynamical models (e.g., Korenaga, 2010), especially considering uncertainties related to mantle hydration and the scaling of bending dissipation for subducting plates (e.g., Rose and Korenaga, 2011; Korenaga, 2011).

The properties of the thermal boundary layer at the base of the mantle determine the core/mantle heat flow. We incorporate a simple boundary-layer model resting on the assumption that convective instability occurs once a local Rayleigh number reaches a critical value. Thus, we calculate the value of Q_{CMB} at any epoch relative to the present (Buffett, 2002):

$$\frac{Q_{CMB}(t_1)}{Q_{CMB}(t_0)} = \left(\frac{T_U(t_1) - T_B(t_1)}{T_U(t_0) - T_B(t_0)}\right)^{\frac{4}{3}} \left(\frac{\eta_B[\overline{T}(t_0)]}{\eta_B[\overline{T}(t_1)]}\right)^{\frac{1}{3}}, \tag{2}$$

where $\overline{T}(t) = [T_U(t) + T_B(t)]/2$ is the average temperature in the thermal boundary layer. Assuming whole-mantle convection as indicated by seismic tomography of slabs and plumes (e.g., van der Hilst et al., 1997; French and Romanowicz, 2015), the temperature at the base of the mantle scales as $T_B(t_1) = [T_M(t_1)/T_M(t_0)]T_B(t_0)$. If convection in the mantle were layered, then T_B would increase by the temperature contrast across the mid-mantle transition layer. Hence, the estimated temperature contrast across the CMB would decrease.

The effective viscosity of the thermal boundary layer is calculated as (Korenaga, 2005)

$$\eta_B(T) = \eta_B(T_{ref}) \exp\left[\frac{H_{eff}}{RT} - \frac{H_{eff}}{RT_{ref}}\right], \tag{3}$$

where H_{eff} is the activation enthalpy, R is the universal gas constant, and $\eta_B(T_{ref})$ is the reference viscosity, comparable to the average viscosity of the lower mantle, at some reference temperature T_{ref}. Typical values assumed for H_{eff} are on the order of ~300 kJ $\mathrm{mol^{-1}}$. But the rheology of the lower mantle is uncertain enough that negative values are also possible, in which case hotter material would have higher viscosity (e.g., Solomatov, 1996; Korenaga, 2005).

Assuming the stagnant layer is in a steady state, the temperature at the top of the stagnant layer is easily calculated (e.g., Turcotte and Schubert, 2002):

$$T_U = T_{CMB} - \frac{Q_{CMB}}{4\pi k_M}\left(\frac{1}{R_C} - \frac{1}{R_S}\right), \tag{4}$$

where T_{CMB} is the temperature at the top of the core, k_M is the thermal conductivity of the lower mantle, and $R_S = R_C + d_S$ is the distance from the center of Earth to the top of the stagnant layer. The effective thickness of the stagnant layer is d_S. Small changes to d_S (<10 km) are degenerate with the slight decrease in T_U caused by plausible rates of radiogenic heating in the stagnant layer, which we neglect.

2.2. Energetics of the core

The global energy balance for the core is (e.g., Labrosse, 2015):

$$Q_{CMB} = Q_R + Q_S + Q_P + Q_G + Q_L, \tag{5}$$

where Q_R is radiogenic heating and Q_S is secular cooling. Gravitational energy associated with the precipitation of magnesium-bearing minerals is Q_P (e.g., Buffett et al., 2000; O'Rourke and Stevenson, 2016). The final two terms are the gravitational energy (Q_G) and latent heat (Q_L) associated with the growth of the inner core. Note that the ohmic dissipation of the dynamo is not included here, because such heating is both generated and dissipated entirely within the core. Analytic expressions for all but one term are available in Labrosse (2015), along with associated constants like the density contrast at the inner core boundary and the slopes of the liquidus and isentropic temperature gradients. We derive a polynomial expression for Q_P in the Appendix. In O'Rourke and Stevenson (2016), we presented an expression for Q_P compatible with the formulation of Nimmo (2015). We use the fourth-order expansion of Labrosse (2015) in this paper for a better match to the density structure of the core from PREM and estimates of the heat gradients at the top of the core.

We approximate the thermal conductivity within the core using a quadratic polynomial (Labrosse, 2015):

$$k_C(r) = k_C(0)\left(1 - A_k \frac{r^2}{L_p^2}\right), \tag{6}$$

where r is radial distance, L_p is derived from the equation of state for the liquid core alloy, and A_k is a constant. According to most recent studies, the thermal conductivity at the center of the core is $k_C(0) \approx 163$ W m^{-1} K^{-1} (e.g., Labrosse, 2015). But we run some simulations using values as low as 40 W m^{-1} K^{-1} (Konôpková et al., 2016).

Each of the terms besides Q_R are proportional to the cooling rate of the core. That is,

$$Q_{CMB} = Q_R + (\widetilde{Q}_S + \widetilde{Q}_P + \widetilde{Q}_G + \widetilde{Q}_L)\frac{dT_{CMB}}{dt}, \tag{7}$$

where $\widetilde{Q}_i = Q_i/(dT_{CMB}/dt)$. The growth rate of the inner core is simply proportional to the overall cooling rate as $dR_I/dt = \gamma_I(dT_{CMB}/dt)$. Here, we use a conversion factor (Nimmo, 2015):

$$\gamma_I = \frac{-1}{\frac{dT_m}{dP} - \frac{dT_a}{dP}}\left(\frac{T_I}{g\rho_I T_{CMB}}\right), \tag{8}$$

where dT_m/dP and dT_a/dP are the slopes of the melting curve and adiabatic temperature gradient, respectively, at the inner core boundary. Likewise, T_I and ρ_I are the temperature and density at the inner core boundary calculated from the adiabatic profiles in Labrosse (2015).

Another equation expresses the conservation of entropy production (e.g., Gubbins, 1977; Labrosse, 2015):

$$\frac{Q_{CMB}}{T_{CMB}} = \frac{Q_R}{T_R} + \frac{Q_S}{T_S} + \frac{Q_L}{T_L} + E_K + E_\phi, \tag{9}$$

where T_R, T_S, and T_L are effective temperatures at which the respective heat sources are dissipated. The entropy production rates associated with conductive heat transport along the adiabatic temperature gradient and ohmic dissipation are E_K and E_ϕ, respectively.

Rearranging Eq. (7), the cooling rate of the core is

$$\frac{dT_{CMB}}{dt} = \frac{Q_{CMB} - Q_R}{\widetilde{Q}_S + \widetilde{Q}_P + \widetilde{Q}_G + \widetilde{Q}_L}. \tag{10}$$

Combining Eqs. (7) and (9), we finally calculate the entropy available to sustain the dynamo

$$E_\phi = \frac{Q_{CMB}}{T_{CMB}} - \frac{Q_R}{T_R} - \left(\frac{\widetilde{Q}_S}{T_S} + \frac{\widetilde{Q}_L}{T_L}\right)\frac{dT_{CMB}}{dt} - E_K. \tag{11}$$

To sustain a dynamo, E_ϕ must of course be positive. Something in the rather wide range of ~20–500 MW K^{-1} is probably required, and the actual minimum value is poorly constrained because ohmic dissipation occurs at short length scales that are difficult to simulate (e.g., Gubbins, 1977). We can estimate the energy associated with ohmic dissipation as $Q_\phi = T_\phi E_\phi$, where $T_\phi \approx 5000$ K is some characteristic temperature of dissipation between T_{CMB} and the temperature at the inner core boundary (Nimmo, 2015). The dissipation rate is an acceptable proxy for magnetic field strength, although more complicated scaling laws have been formulated (e.g., Christensen, 2010).

Only a portion of core formation occurred in the aftermath of giant impacts. Since the equilibration temperature for most material was <4500 K, the core was likely undersaturated in light elements at first, assuming full mixing and an initially homogeneous core. Thus, precipitation of magnesium-bearing minerals was delayed until after an initial episode of cooling (O'Rourke and Stevenson, 2016; Badro et al., 2016). Once started, however, precipitation continues until the core is entirely depleted in light elements. Here we assume that precipitation has been occurring for the entire length of our simulations, meaning that the core became saturated within ~500 Myr after accretion.

Based on diamond-anvil cell experiments conducted at extreme temperature/pressure conditions, Badro et al. (2016) determined that pure MgO would precipitate at a rate $C_M \approx 2.5 \times 10^{-5}$ K^{-1} normalized to the total mass of the core. O'Rourke and Stevenson (2016) included SiO_2 and FeO in the precipitate and did not assume the core and mantle were in equilibrium after accretion, yielding a larger $C_M \approx 5 \times 10^{-5}$ K^{-1}. These calculations were based on extrapolations of earlier experiments conducted at lower temperatures, but Badro et al. (2016) obtained roughly consistent expressions for the relevant exchange coefficients. Entropic arguments suggest that the precipitate should include every element present in the outer core. Because Mg is least soluble, the precipitate is initially MgO-rich but contains increasing amounts of SiO_2 as T_{CMB} decreases. The initial abundances of each element—several combinations of which satisfy constraints from seismology and mineral physics (e.g., Badro et al., 2014; Fischer et al., 2015)—dictate the evolving composition of the precipitate. Given the myriad uncertainties, we use the intermediate value $C_M = 4 \times 10^{-5}$ K^{-1} for most simulations but also describe the implications of higher or lower values.

If E_ϕ is assumed to have been roughly constant throughout geologic time, then we can modify the above equations to calculate the implied values of Q_{CMB} and T_{CMB} in the past (e.g., O'Rourke and Stevenson, 2016). However, since mantle dynamics actually control Q_{CMB} and thus T_{CMB} as detailed above, using Eq. (11) and a coupled model of core/mantle evolution is required to determine what scenarios are compatible with the observed longevity of Earth's dynamo.

2.3. Calculating thermochemical histories

Various observational constraints on the thermal budget of Earth today are available. The total heat flux at the surface is 44 ± 3 TW (Jaupart et al., 2007). Estimates of the present-day heat production in the bulk silicate Earth range from 16 ± 3 TW (Lyubetskaya and Korenaga, 2007) to ~20 TW (Jaupart et al., 2007). Arguments from mineral physics and seismology have implied that the core/mantle boundary heat flow is currently ~5 to 15 TW (e.g., Lay et al., 2008). With heat production in the continental crust estimated as ~6 to 8 TW (Jaupart et al., 2007), radiogenic heating in the mantle is perhaps ~6 to 14 TW and reasonable values for the mantle heat flux might be ~33 to 41 TW. Experiments on metal-silicate partitioning suggest that the abundance of potassium in the core is less than 200 ppm (e.g., Corgne et al., 2007), implying that radiogenic heating in the core is <1.5 TW at present.

Absolute temperatures within Earth now are comparably uncertain. Extrapolating temperatures of the relevant phase transitions at the mantle's transition zone down an adiabatic gradient imply that the basal temperature of the mantle is ~2500 to 2800 K. With a present-day temperature of ~4000 K at the top of the core (Labrosse, 2015), the temperature contrast across the core/mantle boundary is ~1000 to 1800 K, much larger than the thermal excess of <500 K attributed to mantle plumes (e.g., French and Romanowicz, 2015). Note that this thermal excess may diminish by a factor of roughly two as plumes ascend from the CMB to the upper mantle. That is, a near-surface thermal excess of ~250 K may imply a temperature difference of ~500 K across the thermal boundary layer at the base of the mantle (e.g., Leng and Zhong, 2008).

Using the present as an "initial" condition, we can integrate the equations presented above backwards in time to calculate a thermochemical history of Earth. The present-day thermal budget has significant uncertainties, but constraints on the state of the mantle and core at the time that plate tectonics began are obvi-

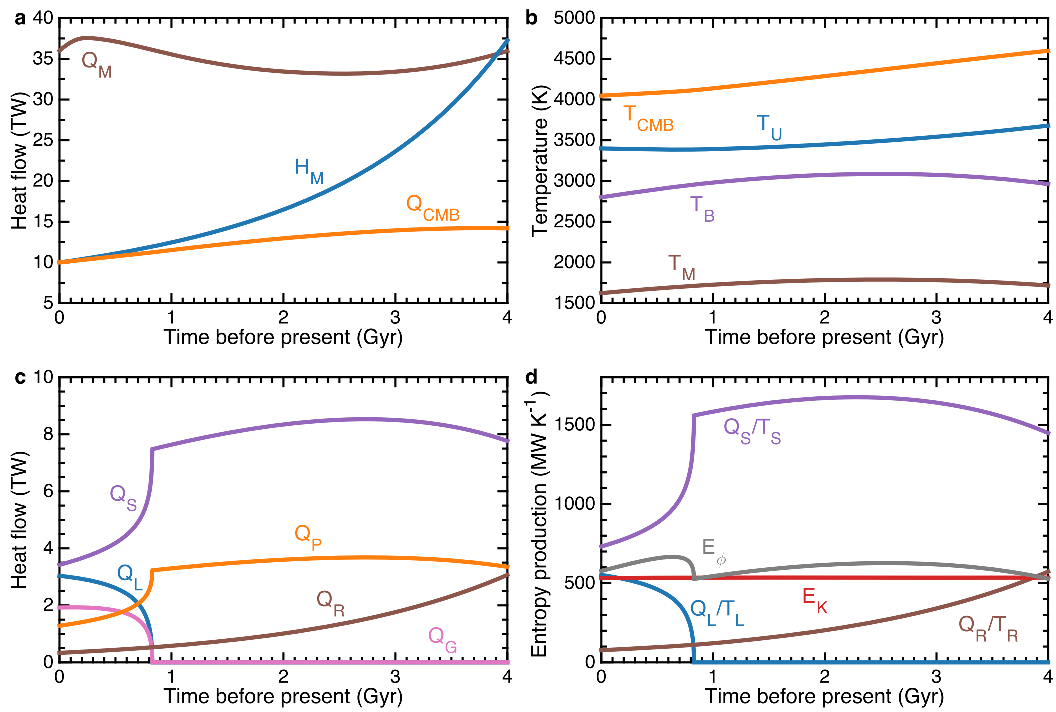

Fig. 2. Simulation of the thermal evolution of Earth with nominal initial conditions: $k_C(0) = 163$ W m^{-1} K^{-1}, $Q_M(t_0) = 36$ TW, $Q_{CMB}(t_0) = 10$ TW, $H_M(t_0) = 10$ TW, $H_{eff} = 300$ kJ mol^{-1}, $d_S = 50$ km, and [K] = 50 ppm. Magnesium-bearing minerals precipitate from the core at a rate of $C_M = 4 \times 10^{-5}$ K^{-1}. (a) Heat budget of the mantle. (b) Temperatures of the mantle and core. Contributions to the energy (c) and entropy (d) budgets of the core.

ously much weaker. This procedure may not reproduce the state of the core and mantle throughout the Hadean because scaling laws other than those presented above or more complicated numerical simulations are required to model the aftermath of giant impacts, the solidification of the primordial magma ocean, and any regime of mantle dynamics that may have preceded plate tectonics. Accordingly, the primary utility of our approach is to reconstruct a thermal history for the mantle consistent with geologic evidence for the period when the geodynamo definitely existed.

In every simulation, we assume that $T_B(t_0) = 2800$ K and that continents grew to their modern size by 4 Ga. Using the adiabatic temperature gradient for the core from Labrosse (2015) implies that $T_{CMB} \approx 4050$ K given the present-day radius of the inner core, R_I = 1220 km. Unless otherwise indicated, we use the following set of "nominal" parameters: $Q_M(t_0) = 36$ TW, $Q_{CMB}(t_0) = 10$ TW, $H_M(t_0) = 10$ TW, $H_{eff} = 300$ kJ mol^{-1} and [K] = 50 ppm in the core. With 8 TW of radiogenic heating in the continental crust in this case, the present-day heat flow thus totals 44 TW. We also assume that the effective thickness of the stagnant layer, $d_S = 50$ km, except when $Q_{CMB}(t_0)$ is varied.

3. Results

Fig. 2 shows the results of the thermal evolution simulation using our nominal parameters. With the rate of magnesium precipitation $C_M = 4 \times 10^{-5}$ K^{-1} (normalized to the total mass of the core), $E_\phi > 500$ MW K^{-1} at all times. The entropy production rises to maxima of ∼670 and 630 MW K^{-1} near 0.65 and 2.5 Ga, respectively, equivalent to ohmic dissipation rates of $Q_\phi \approx$ 3.1–3.4 TW that are well above the minimum estimated to sustain a dynamo (e.g., Nimmo, 2015). The age of the inner core is ∼0.83 Ga, at which point Q_L and Q_G disappear and the entropy production rate reaches a local minimum. At present day, the temperature differences across the thermal boundary layer and the adjacent stagnant layer are both ∼600 K, which roughly matches constraints on the thermal excess associated with mantle plumes and the total temperature contrast across the core/mantle boundary. For the entire simulation, the change in entropy content associated with thermal conduction is as large as the total entropy production available for the dynamo (i.e., $E_K \approx E_\phi$). Precipitation is critical to the operation of a dynamo before inner core nucleation, even though $Q_P \sim 0.5 Q_S$. That is, the contribution of secular cooling to the total dissipation is penalized by a Carnot-like efficiency term $\sim (T_S - T_{CMB})/T_{CMB}$ relative to compositional buoyancy from precipitation or the inner core (Nimmo, 2015; Labrosse, 2015).

Fig. 3 illustrates the effects of varying the rate of magnesium precipitation. Five simulations were performed with C_M increasing from 0 to 8×10^{-5} K^{-1} in increments of 2×10^{-5} K^{-1}. Increasing C_M yields increased entropy production rates, along with decreased Q_{CMB} and T_{CMB} in the past. At least some precipitation is required to maintain positive values of E_ϕ before nucleation of the inner core. Moreover, values of $C_M \geq 4 \times 10^{-5}$ K^{-1} are preferred because E_ϕ must be significantly larger than zero to sustain a global magnetic field (e.g., Nimmo, 2015). Magnesium precipitation notably limits the extent to which E_ϕ, and thus presumably the strength of Earth's magnetic field recorded at the surface, reaches a local minimum at the time of inner core nucleation. That is, entropy production rates are roughly constant within ∼10% throughout geologic time in simulations with $C_M \gtrsim 4 \times 10^{-5}$ K^{-1}.

We repeated the simulations shown in Fig. 3 with the thermal conductivity decreased from $k_C(0) = 163$ to 40 W m^{-1} K^{-1}. With all other parameters held constant, E_K is the only term affected. Thus, the evolution of Q_{CMB} and T_{CMB} is unchanged, while E_ϕ is increased by ∼400 MW K^{-1} at all times. If the lowest estimates of thermal conductivity are actually correct (Konôpková et al., 2016), then magnesium precipitation is not required to maintain positive dissipation. However, at least $C_M = 2 \times 10^{-5}$ is still necessary to unambiguously sustain a dynamo with $E_\phi > 500$ MW K^{-1} at all times.

Fig. 4 elucidates how varying the mantle heat flow affects the evolution of the core. Simulations were performed with $Q_M(t_0)$

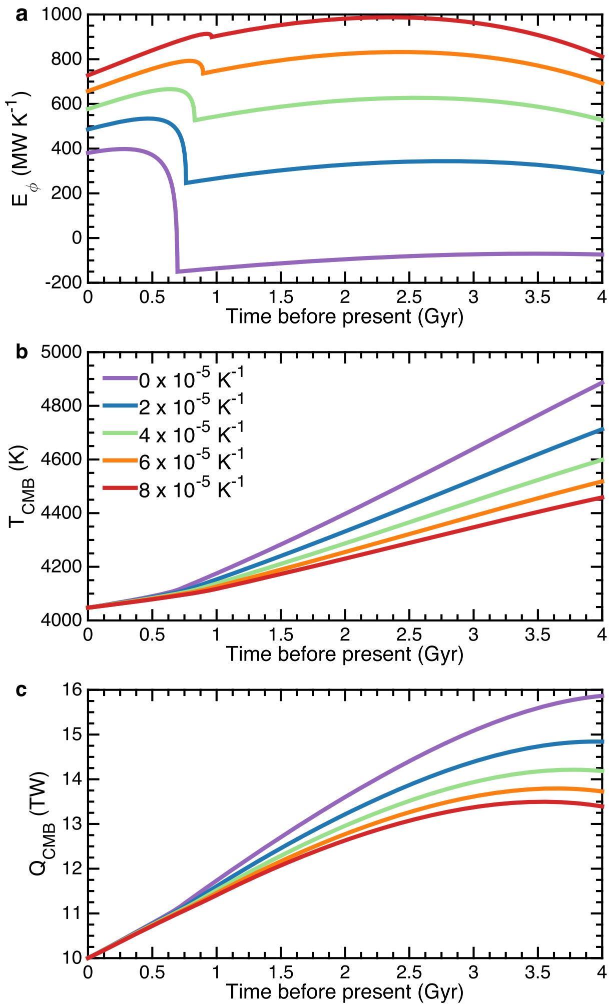

Fig. 3. Multiple simulations showing that increasing the precipitation rate of magnesium-bearing minerals increases the entropy production for the dynamo (a) and, relative to the present, decreases the implied temperatures of the core (b), core/mantle heat flow (c) in the past.

varied from 32 to 40 TW to represent the uncertainties in the thermal budget of Earth. In each of these simulations, $C_M = 4 \times 10^{-5}$ K^{-1}, $H_M(t_0) = 10$ TW, and 8 TW of radiogenic heating is assumed for the continental crust. Increasing $Q_M(t_0)$ implies more entropy production for the dynamo in the past, along with higher values of both Q_M and T_M. The effect on the dynamics of the core, however, is relatively small compared to the uncertainties centered on the other parameters described above. In these simulations, the present-day Urey ratio is ∼0.3, increasing to ∼1–1.2 at 4 Ga. However, using a high present-day Urey ratio (∼0.75), together with conventional scaling laws for mantle dynamics, would only marginally affect our results, at least during the few billion years before the "thermal catastrophe" renders the mantle globally molten.

Fig. 5 contains tests of the sensitivity of our simulations to three additional parameters. Each simulation has $C_M = 4 \times 10^{-5}$ K^{-1} so that positive dissipation is maintained in most cases. Decreasing C_M to 2.5×10^{-5} K^{-1} only lowers the estimated entropy production rates by ∼100 MW K^{-1} at all times. Conventional scalings have the viscosity of the lower mantle decreasing with increasing temperature (e.g., Buffett, 2002). In this case, the CMB heat flow is higher in the past. If $H_{eff} = 300$ kJ mol^{-1}, the implied value is almost 15 TW at 4 Ga for $Q_{CMB}(t_0) = 10$ TW. Attaining more than twice the present-day CMB heat flow in the past is difficult, requiring $H_{eff} \geq 600$ kJ mol^{-1} and the absence of any compositionally-distinct, stagnant layer.

The rheology of the lower mantle is poorly constrained. If the grain size-dependent part of diffusion creep dominates, then hotter mantle may actually have higher viscosity (Solomatov, 1996; Korenaga, 2005). In simulations with negative values of H_{eff}, hotter temperatures in the past would imply a thicker thermal boundary layer at the base of the mantle, leading to inhibited Q_{CMB} and thus a lower likelihood of sustaining a dynamo. With $H_{eff} = -300$ kJ mol^{-1}, the viscosity contrast across the thermal boundary layer is roughly one order of magnitude as long as a stagnant, compositionally-distinct layer with $d_S = 50$ km is still present. If H_{eff} were even more negative, however, then the viscosity contrast may become large enough that the bottom portion of the thermal boundary layer would itself stagnate, despite its compositional homogeneity (e.g., Solomatov and Moresi, 2000). In this case, calculating Q_{CMB} is more complicated (Korenaga, 2005), and a compositionally distinct layer is not required to explain the different thermal excesses associated with the CMB and mantle plumes.

Rates of entropy production are very sensitive to the present-day core/mantle heat flow. To maintain roughly equal differences in temperature across the lower thermal boundary layer for the simulations in Fig. 5, we vary d_S from 72 km for $Q_{CMB}(t_0) = 5$ TW to 38 km for $Q_{CMB}(t_0) = 15$ TW in equal increments of 12 km per 5 TW. If $Q_{CMB}(t_0)$ is ∼5 TW, at the lower end of modern estimates, then even $C_M = 5 \times 10^{-5}$ K^{-1} is insufficient to sustain positive dissipation. Without precipitation, $E_\phi \approx 100$–150 MW K^{-1} before the inner core nucleates if $Q_{CMB}(t_0) = 15$ TW, [K] = 0 ppm, and $H_{eff} = 300$ kJ mol^{-1}. However, higher dissipation rates are likely required to produce the present-day magnetic field strength (Nimmo, 2015). Decreasing $Q_{CMB}(t_0)$ implies that values of Q_{CMB} are depressed by roughly the same amount in the past and also that the inner core is older.

Increased abundances of potassium in the core imply lower rates of ohmic dissipation in the past. This result may seem counterintuitive because radiogenic heating is a positive source of energy and entropy—albeit an inefficient one because of another Carnot-like efficiency term. Calculations that consider only the thermal evolution of the core demonstrate that increased radioactivity lowers the amount of secular cooling required to sustain a dynamo and thus the temperature of the core in the past, but also necessitates a higher core/mantle heat flow (e.g., Nimmo, 2015; Labrosse, 2015; O'Rourke and Stevenson, 2016). There is no reason, however, that Q_{CMB} should increase because of radiogenic heating in the core. In fact, the relatively slow cooling implied by such heating tends to decrease Q_{CMB} by lowering the temperature contrast across the core/mantle boundary. Fundamentally, the rheology of the lower mantle governs Q_{CMB}. Any given value of Q_{CMB} will yield more entropy for a dynamo if cooling causes inner core growth or precipitation rather than just removing heat from the decay of potassium or other radioactive isotopes of uranium and thorium.

We also repeated these sensitivity tests using the lower bound on thermal conductivity. With $k_C(0) = 40$ W m^{-1} K^{-1}, positive dissipation is always maintained for each value of H_{eff}, $Q_{CMB}(t_0)$, and [K] even absent precipitation. Low thermal conductivity also permits $E_\phi \approx 400$ MW K^{-1} when $Q_{CMB}(t_0) = 5$ TW and $C_M = 4 \times 10^{-5}$ K^{-1}. If $Q_{CMB}(t_0) = 5$ TW with low thermal conductivity but no precipitation, then $E_\phi \approx 100$ MW K^{-1} in the past and rises to ∼300 MW K^{-1} when the inner core nucleates at ∼1.4 Gyr before today. Increasing $Q_{CMB}(t_0)$ to 15 TW then yields ∼500 and 1250 MW K^{-1} of entropy production prior to and following the nucleation of the inner core, respectively.

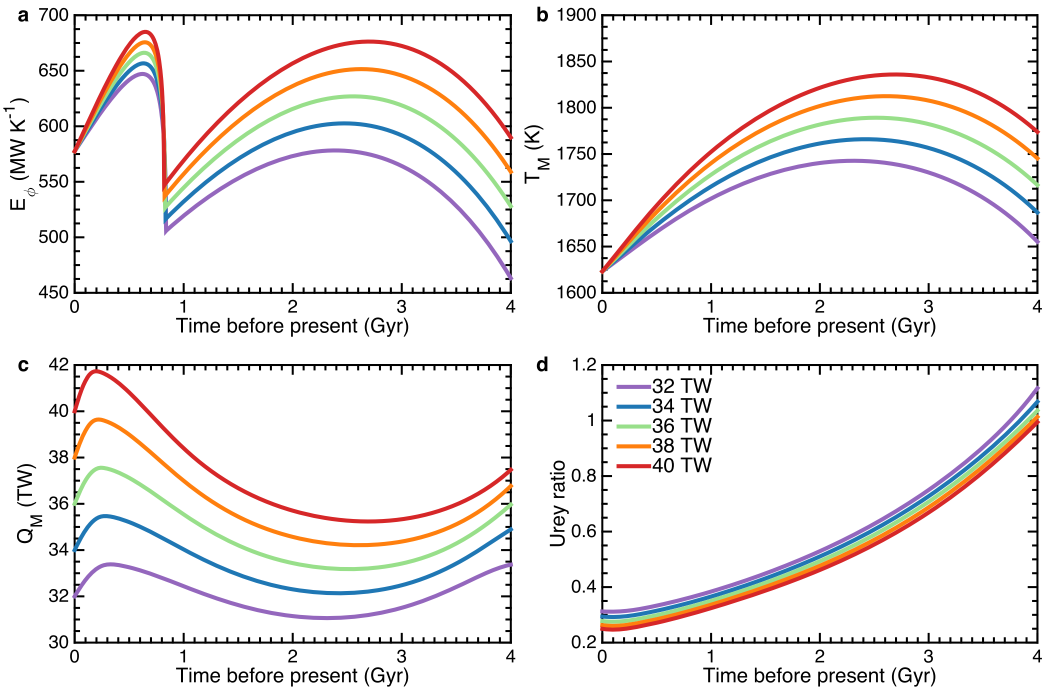

Fig. 4. Simulations showing that increasing the mantle heat flow implies increased rate of entropy production available for the dynamo in the past (a), potential temperature of the mantle (b), and heat flow from the mantle to the surface (c), while the Urey ratio (d) is decreased.

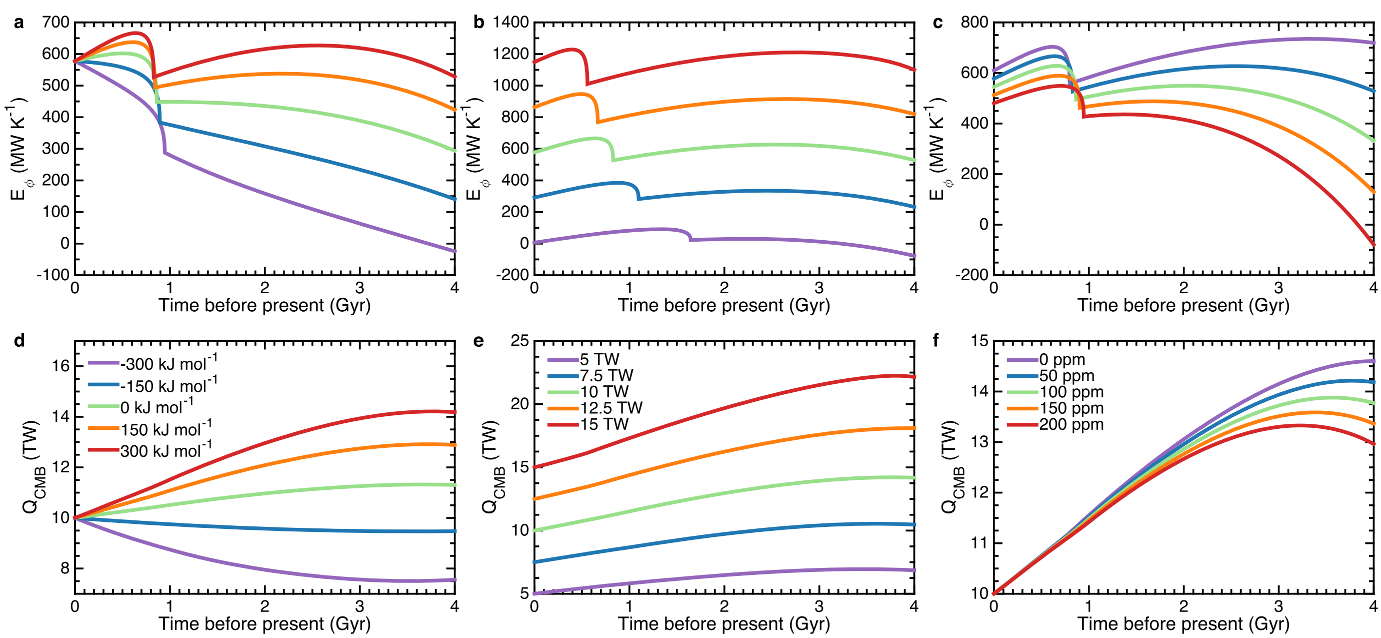

Fig. 5. Simulations with H_{eff} varied from -300 to 300 kJ mol^{-1} (left), $Q_{CMB}(t_0)$ from 5 to 15 TW (center), and [K] from 0 to 200 ppm (right). Top: Rate of entropy production available for the dynamo. Bottom: Heat flow across the core/mantle boundary.

4. Discussion

4.1. Earth's initially hot state

The final stage of Earth's formation featured a number of violent collisions, notably including the Moon-forming impact, that would have at least partially melted the mantle (e.g., Rubie et al., 2015). Even absent giant impacts, the gravitational energy associated with accretion is large enough to create temperatures in the core and mantle much higher than those prevailing today. Without high temperatures at the time of core formation, insufficient magnesium would partition into the core to provide an appreciable amount of compositional buoyancy during its later evolution (Wahl and Militzer, 2015; O'Rourke and Stevenson, 2016; Badro et al., 2016). If extrapolated backwards until the time of Earth's accretion, however, our scalings of plate tectonics predict that the mantle was not much hotter than it is today. Efficient heat loss from a vigorously convecting magma ocean must have actually occurred after accretion. We have not explicitly included a period of rapid cooling before the initiation of plate tectonics, so our simulations may not be representative of Earth's earliest history.

Assuming that plate tectonics operated throughout the Proterozoic is quite reasonable (e.g., Korenaga, 2013), and our central goal is explaining how Earth sustained a dynamo throughout this eon. Observational evidence for the operation of plate tectonics is lacking for the same reason—a scarcity of rocks—that the existence of a magnetic field in the deep past remains controversial. Calculations in this paper and fully dynamical simulations using the new scaling for plate tectonics suggest that the potential temperature of the mantle was ∼1800 K at >3 Ga (Herzberg et al., 2010; Korenaga, 2011). Crucially, this is within ∼100 K of the potential temperature necessary for a surface magma ocean (e.g., Rubie et al., 2015), meaning that our simulations of plate tectonics should smoothly connect with models that describe the solidification of a magma ocean and possibly another, short-lived regime of mantle convection (e.g., Moore and Webb, 2013).

A magma ocean extending from the surface through the transition zone to 660 km depth would have existed when the potential temperature was ∼2200–2300 K (e.g., Rubie et al., 2015). Subsequently cooling the mantle by ∼400 K over 1 Gyr, for example, to the state when plate tectonics may have begun requires $Q_M \sim 100$ TW from the magma ocean, more than twice the heat flow associated with solid-state convection. Of course, the actual lifespan of the surface magma ocean, which could be much shorter than 1 Gyr, is very uncertain (e.g., Solomatov, 2007). Additionally, the temperature of the core may have decreased by ∼1000 K or more during the earliest phase of cooling after Earth's "hot start." After this initial burst, a long-lived magma ocean at the base of the mantle may have delayed the onset of the geodynamo. That is, the core would not continue cooling below the liquidus temperature of the mantle melt until the basal magma ocean solidified (Labrosse et al., 2007). Discovering whether a global magnetic field existed throughout the Archean and Hadean would provide critical constraints on these processes.

4.2. Limitations of our modeling approach

Using one-dimensional scaling laws to describe the coupled evolution of Earth's core and mantle is computationally efficient and allows for rapid sensitivity tests and description of first-order phenomena (e.g., Stevenson et al., 1983; Christensen, 1985). Future work, however, should address some shortcomings of our approach. Parameterizations of core energetics coupled to fully dynamical simulations of the mantle (e.g., Nakagawa and Tackley, 2010) should include precipitation of magnesium-bearing minerals. If CMB heat flow is sub-adiabatic and no compositional buoyancy is available (e.g., before the nucleation of the inner core absent precipitation), then additional equations are required to model the dynamics in the presence of a thick, stable layer at the top of the core since only part of the outer core would vigorously convect (e.g., Labrosse, 2015). We have neglected this complication because such scenarios are probably not compatible with the observed longevity of the global magnetic field.

More importantly, the CMB is both spatially and temporally heterogeneous in terms of composition and temperature. The stagnant layer in our models condenses vertical and lateral variations such as the post-perovskite phase transition and double-crossings, along with regions like large low-shear-wave-velocity provinces and ultralow-velocity zones (e.g., Hernlund and McNamara, 2015). The spatial variability of CMB heat flow caused by cold slabs, in particular, may control the timing of geomagnetic reversals (e.g., Olson et al., 2013). Fluid motions associated with baroclinic instability can drive lateral transport of heat and assist the operation of a dynamo. The associated entropy production, however, is likely small because the effective temperature of dissipation is close to that of the CMB, reducing its Carnot-like efficiency (e.g., Labrosse, 2015). Thus, we have not included any parameterization of this process.

4.3. Implications for Venus

Spacecraft have constrained the magnetic moment on Venus to less than 10^{-5} times the terrestrial value (Phillips and Russell, 1987). Although its moment of inertia is presently unknown, assuming that Venus has an iron-rich core like Earth seems reasonable. Thermal evolution models imply that the core of Venus would not have frozen completely solid (e.g., Stevenson et al., 1983), but convection must have ceased in the liquid portion for some reason. Jacobson et al. (2015) proposed that Venus did not suffer a giant impact, in which case a stable stratification would develop as the concentration of light elements in material added to the top of the core increased with pressure/temperature conditions during accretion. No giant impact also means no magnesium to precipitate and provide energy and entropy for the dynamo. Future work should consider estimates of the CMB heat flow from, for example, thermal evolution models (e.g., Nimmo, 2002; O'Rourke and Korenaga, 2015) and the buoyancy flux of mantle plumes (e.g., Smrekar and Sotin, 2012). Estimates above the critical value required to drive a dynamo in a mostly isentropic and homogeneous core would serve as evidence that the core of Venus was indeed initially stratified.

5. Conclusions

Simple scalings for mantle dynamics, along with a parametrized model for the energetics of the core, allow us to estimate how much entropy has been available to sustain a dynamo throughout geologic time. If the recent upward revision of the thermal conductivity of the core is correct, then the precipitation of magnesium-bearing minerals at rates suggested by O'Rourke and Stevenson (2016) and Badro et al. (2016) allows vigorous convection prior to the nucleation of the inner core for most combinations of initial conditions. Ongoing precipitation would produce positive rates of entropy production for at least 3.45 Gyr as long as the abundance of potassium is under ∼200 ppm and the present-day CMB heat flow is above ∼5 TW. Because the minimum required heat flow across the core/mantle boundary remains roughly constant, the longevity of the magnetic field is compatible with a weak dependence of mantle heat flow on temperature. Precipitation may yield roughly constant rates of entropy production over time, meaning that inner core's formation may not create a dramatic increase in field strength preserved in the paleomagnetic record. Similar computational exercises are relevant to Venus and probably differentiated "super-Earth" exoplanets.

Acknowledgements

This material is based upon work supported by the National Science Foundation Graduate Research Fellowship under Grant No. DGE-1144469. Thanks to John Hernlund, Jonathan Aurnou, and Roger Fu for helpful discussions. An anonymous reviewer provided many helpful comments that improved this manuscript.

Appendix A. Derivation of Q_P

The release of gravitational energy associated with the precipitation of magnesium-bearing minerals is easily defined if the rate of precipitation is roughly constant (O'Rourke and Stevenson, 2016)

$$Q_P = -\int_{\infty} \rho(r)\psi(r)\beta_M C_M \frac{dT_{CMB}}{dt} dV, \tag{A.1}$$

where C_M is the fraction of the core's mass precipitated per 1 K of cooling and ρ is the density profile in the core. Since precipitation only occurs out of the liquid portion of the core

$$Q_P = -\left[\int\limits_{OC} \rho(r)\psi(r)dV - M_{OC}\psi(R_I)\right]\beta_M C_M \frac{dT_{CMB}}{dt}, \quad \text{(A.2)}$$

where OC refers to the outer core and R_I is the radius of the inner core.

The coefficient of compositional expansion associated with magnesium precipitate is

$$\beta_M = -\frac{1}{\rho}\left(\frac{\partial\rho}{\partial\xi}\right)_{P,T}, \quad \text{(A.3)}$$

where ξ is the concentration of magnesium-rich material. Assuming that the density change between the precipitate and the residual core alloy is roughly equal to that across the core/mantle boundary, then $\beta_M \sim 0.8$. This value is probably only accurate within several tens of percents, but our uncertainty about the value of C_M is much larger and degenerate.

The gravitational potential in the core relative to zero potential at the CMB is

$$\psi(R) = \left[\frac{2}{3}\pi G\rho_0 r^2\left(1 - \frac{3}{10}\frac{r^2}{L_p^2} - \frac{A_p}{7}\frac{r^4}{L_p^4}\right)\right]\Bigg|_{R_C}^{R}, \quad \text{(A.4)}$$

where ρ_0 is the central density and A_p and L_p are defined in Labrosse (2015) based on the equation of state of liquid core alloy. Since this and the density profile are both available as polynomials, we can write an analytic equation

$$\begin{aligned} Q_P = -\beta_M C_M \Bigg\{ \frac{8}{3}\pi^2 G\rho_0^2 \Bigg[-\frac{\Gamma}{3}r^3 + \frac{2}{10}\left(1 + \frac{\Gamma}{L_p^2}\right)r^5 \\ + \frac{1}{7L_p^2}\left(\frac{A_p\Gamma}{L_p^2} - \frac{13}{10}\right)r^7 + \frac{1}{9L_p^4}\left(\frac{3}{10} - \frac{8A_p}{7}\right)r^9 \quad \text{(A.5)} \\ + \frac{31A_p}{770L_p^6}r^{11} + \frac{A_p^2}{91L_p^8}r^{13}\Bigg]\Bigg|_{R_I}^{R_C} - \Gamma M_{OC}\Bigg\}\frac{dT_{CMB}}{dt}, \end{aligned}$$

where

$$\Gamma = R_C^2\left(1 - \frac{3}{10}\frac{R_C^2}{L_p^2} - \frac{A_p}{7}\frac{R_C^4}{L_p^4}\right). \quad \text{(A.6)}$$

References

Badro, J., Cote, A.S., Brodholt, J.P., 2014. A seismologically consistent compositional model of Earth's core. Proc. Natl. Acad. Sci. 111, 7542–7545.
Badro, J., Siebert, J., Nimmo, F., 2016. An early geodynamo driven by exsolution of mantle components from Earth's core. Nature, 1–3.
Biggin, A.J., Piispa, E.J., Pesonen, L.J., Holme, R., Paterson, G.A., Veikkolainen, T., Tauxe, L., 2015. Palaeomagnetic field intensity variations suggest Mesoproterozoic inner-core nucleation. Nature 526, 245–248.
Biggin, A.J., de Wit, M.J., Langereis, C.G., Zegers, T.E., Voûte, S., Dekkers, M.J., Drost, K., 2011. Palaeomagnetism of Archaean rocks of the Onverwacht Group, Barberton Greenstone Belt (southern Africa): evidence for a stable and potentially reversing geomagnetic field at ca. 3.5 Ga. Earth Planet. Sci. Lett. 302, 314–328.
Buffett, B.A., 2002. Estimates of heat flow in the deep mantle based on the power requirements for the geodynamo. Geophys. Res. Lett. 29, 1566.
Buffett, B.A., Garnero, E.J., Jenaloz, R., 2000. Sediments at the top of Earth's core. Science 290, 1338–1342.
Christensen, U.R., 1985. Thermal evolution models for the Earth. J. Geophys. Res. 90, 2995.
Christensen, U.R., 2010. Dynamo scaling laws and applications to the planets. Space Sci. Rev. 152, 565–590.
Corgne, A., Keshav, S., Fei, Y., McDonough, W.F., 2007. How much potassium is in the Earth's core? New insights from partitioning experiments. Earth Planet. Sci. Lett. 256, 567–576.
Farnetani, C.G., 1997. Excess temperature of mantle plumes: the role of chemical stratification across D″. Geophys. Res. Lett. 24, 1583–1586.
Fischer, R.A., Nakajima, Y., Campbell, A.J., Frost, D.J., Harries, D., Langenhorst, F., Miyajima, N., Pollok, K., Rubie, D.C., 2015. High pressure metal–silicate partitioning of Ni, Co, V, Cr, Si and O. Geochim. Cosmochim. Acta 167, 177–194.
French, S.W., Romanowicz, B., 2015. Broad plumes rooted at the base of the Earth's mantle beneath major hotspots. Nature 525, 95–99.
Gomi, H., Ohta, K., Hirose, K., Labrosse, S., Caracas, R., Verstraete, M.J., Hernlund, J.W., 2013. The high conductivity of iron and thermal evolution of the Earth's core. Phys. Earth Planet. Inter. 224, 88–103.
Gubbins, D., 1977. Energetics of Earth's core. J. Geophys. 43, 453–464.
Hernlund, J., McNamara, A., 2015. The core–mantle boundary region. In: Treatise on Geophysics. Elsevier B.V., pp. 461–519.
Herzberg, C., Condie, K., Korenaga, J., 2010. Thermal history of the Earth and its petrological expression. Earth Planet. Sci. Lett. 292, 79–88.
van der Hilst, R.D., Widiyantoro, S., Engdahl, E.R., 1997. Evidence for deep mantle circulation from global tomography. Nature 386, 578–584.
Jacobson, S.A., Rubie, D.C., Hernlund, J., Morbidelli, A., 2015. A late giant impact is necessary to create Earth's magnetic field. In: LPSC Abstracts, p. 1882.
Jaupart, C., Labrosse, S., Mareschal, J.C., 2007. Temperatures, heat and energy in the mantle of the Earth. In: Treatise on Geophysics. Elsevier, pp. 253–303.
de Koker, N., Steinle-Neumann, G., Vlcek, V., 2012. Electrical resistivity and thermal conductivity of liquid Fe alloys at high P and T, and heat flux in Earth's core. PNAS 109, 4070–4073.
Konôpková, Z., McWilliams, R.S., Gómez-Pérez, N., Goncharov, A.F., 2016. Direct measurement of thermal conductivity in solid iron at planetary core conditions. Nature 534, 99–101.
Korenaga, J., 2005. Firm mantle plumes and the nature of the core–mantle boundary region. Earth Planet. Sci. Lett. 232, 29–37.
Korenaga, J., 2006. Archean geodynamics and the thermal evolution of Earth. Arch. Geodyn. Environ. 164, 7–32.
Korenaga, J., 2008. Urey ratio and the structure and evolution of Earth's mantle. Rev. Geophys., 1–32.
Korenaga, J., 2010. Scaling of plate tectonic convection with pseudoplastic rheology. J. Geophys. Res. 115, 1–24.
Korenaga, J., 2011. Thermal evolution with a hydrating mantle and the initiation of plate tectonics in the early Earth. J. Geophys. Res. 116, B12403.
Korenaga, J., 2013. Initiation and evolution of plate tectonics on Earth: theories and observations. Annu. Rev. Earth Planet. Sci. 41, 117–151.
Labrosse, S., 2015. Thermal evolution of the core with a high thermal conductivity. Phys. Earth Planet. Inter. 247, 36–55.
Labrosse, S., Hernlund, J.W., Coltice, N., 2007. A crystallizing dense magma ocean at the base of the Earth's mantle. Nature 450, 866–869.
Labrosse, S., Poirier, J.P., Le Mouël, J.L., 2001. The age of the inner core. Earth Planet. Sci. Lett. 190, 111–123.
Lay, T., Hernlund, J., Buffett, B.A., 2008. Core–mantle boundary heat flow. Nat. Geosci. 1, 25–32.
Leng, W., Zhong, S., 2008. Controls on plume heat flux and plume excess temperature. J. Geophys. Res., Solid Earth 113, 1–15.
Lyubetskaya, T., Korenaga, J., 2007. Chemical composition of Earth's primitive mantle and its variance: 2. Implications for global geodynamics. J. Geophys. Res. 112, B03212.
Moore, W.B., Webb, A.G., 2013. Heat-pipe Earth. Nature 501, 501–505.
Nakagawa, T., Tackley, P.J., 2010. Influence of initial CMB temperature and other parameters on the thermal evolution of Earth's core resulting from thermochemical spherical mantle convection. Geochem. Geophys. Geosyst. 11.
Nimmo, F., 2002. Why does Venus lack a magnetic field? Geology 30, 987.
Nimmo, F., 2015. Energetics of the core. In: Treatise on Geophysics, vol. 1, second edition. Elsevier B.V., pp. 31–65.
Ohta, K., Kuwayama, Y., Hirose, K., Shimizu, K., Ohishi, Y., 2016. Experimental determination of the electrical resistivity of iron at Earth's core conditions. Nature 534, 95–98.
Olson, P., Deguen, R., Hinnov, L.A., Zhong, S., 2013. Controls on geomagnetic reversals and core evolution by mantle convection in the Phanerozoic. Phys. Earth Planet. Inter. 214, 87–103.
O'Rourke, J.G., Korenaga, J., 2015. Thermal evolution of Venus with argon degassing. Icarus 260, 128–140.
O'Rourke, J.G., Stevenson, D.J., 2016. Powering Earth's dynamo with magnesium precipitation from the core. Nature 529, 387–389.
Phillips, J.L., Russell, C.T., 1987. Revised upper limit on the internal magnetic moment of Venus. J. Geophys. Res. 92, 2253–2263.
Pozzo, M., Davies, C., Gubbins, D., Alfè, D., 2012. Thermal and electrical conductivity of iron at Earth's core conditions. Nature 485, 355–358.
Rose, I.R., Korenaga, J., 2011. Mantle rheology and the scaling of bending dissipation in plate tectonics. J. Geophys. Res. 116, B06404.
Rubie, D.C., Jacobson, S., Morbidelli, A., O'Brien, D., Young, E., de Vries, J., Nimmo, F., Palme, H., Frost, D., 2015. Accretion and differentiation of the terrestrial planets with implications for the compositions of early-formed Solar System bodies and accretion of water. Icarus 248, 89–108.
Seagle, C.T., Cottrell, E., Fei, Y., Hummer, D.R., Prakapenka, V.B., 2013. Electrical and thermal transport properties of iron and iron–silicon alloy at high pressure. Geophys. Res. Lett. 40, 5377–5381.
Smirnov, A.V., Tarduno, J.A., Kulakov, E.V., McEnroe, S.A., Bono, R.K., 2016. Palaeointensity, core thermal conductivity and the unknown age of the inner core. Geophys. J. Int. 205, 1190–1195.

Smrekar, S.E., Sotin, C., 2012. Constraints on mantle plumes on Venus: implications for volatile history. Icarus 217, 510–523.
Solomatov, V., 2007. Magma oceans and primordial mantle differentiation. In: Schubert, G. (Ed.), Treatise on Geophysics. Elsevier, pp. 91–119.
Solomatov, V.S., 1996. Can hotter mantle have a larger viscosity? Geophys. Res. Lett. 23, 937–940.
Solomatov, V.S., Moresi, L.N., 2000. Scaling of time-dependent stagnant lid convection: application to small-scale convection on Earth and other terrestrial planets. J. Geophys. Res. 105, 21795–21817.
Stelzer, Z., Jackson, A., 2013. Extracting scaling laws from numerical dynamo models. Geophys. J. Int. 193, 1265–1276.
Stevenson, D.J., 1987. Limits on lateral density and velocity variations in the Earth's outer core. Geophys. J. Int. 88, 311–319.
Stevenson, D.J., 2003. Planetary magnetic fields. Earth Planet. Sci. Lett. 208, 1–11.
Stevenson, D.J., Spohn, T., Schubert, G., 1983. Magnetism and thermal evolution of the terrestrial planets. Icarus 54, 466–489.
Tang, X., Ntam, M.C., Dong, J., Rainey, E.S.G., Kavner, A., 2014. The thermal conductivity of Earth's lower mantle. Geophys. Res. Lett. 41, 2746–2752.
Tarduno, J.A., Cottrell, R.D., Davis, W.J., Nimmo, F., Bono, R.K., 2015. A Hadean to Paleoarchean geodynamo recorded by single zircon crystals. Science 349, 521–524.
Tarduno, J.A., Cottrell, R.D., Watkeys, M.K., Hofmann, A., Doubrovine, P.V., Mamajek, E.E., Liu, D., Sibeck, D.G., Neukirch, L.P., Usui, Y., 2010. Geodynamo, solar wind, and magnetopause 3.4 to 3.45 billion years ago. Science 327, 1238–1240.
Turcotte, D.L., Schubert, G., 2002. Geodynamics. Cambridge University Press, New York.
Wahl, S.M., Militzer, B., 2015. High-temperature miscibility of iron and rock during terrestrial planet formation. Earth Planet. Sci. Lett. 410, 25–33.
Weiss, B.P., Maloof, A.C., Tailby, N., Ramezani, J., Fu, R.R., Hanus, V., Trail, D., Bruce Watson, E., Harrison, T.M., Bowring, S.A., Kirschvink, J.L., Swanson-Hysell, N.L., Coe, R.S., 2015. Pervasive remagnetization of detrital zircon host rocks in the Jack Hills, Western Australia and implications for records of the early geodynamo. Earth Planet. Sci. Lett. 430, 115–128.